

Chimera in a neuronal network model of the cat brain

M. S. Santos¹, J. D. Szezech Jr^{1,2}, F. S. Borges¹, K. C. Iarosz³,

I. L. Caldas³, A. M. Batista^{1,2,3}, R. L. Viana⁴, J. Kurths⁵

¹*Pós-Graduação em Ciências, Universidade Estadual de Ponta Grossa, Ponta Grossa, PR, Brazil.*

²*Departamento de Matemática e Estatística, Universidade Estadual de Ponta Grossa, Ponta Grossa, PR, Brazil.*

³*Instituto de Física, Universidade de São Paulo, São Paulo, SP, Brazil.*

⁴*Departamento de Física, Universidade Federal do Paraná, Curitiba, PR, Brazil.*

⁵*Department of Physics, Humboldt University, Berlin,*

Germany; Institute for Complex Systems and Mathematical Biology, Aberdeen, Scotland; and Potsdam Institute for Climate Impact Research, Potsdam, Germany.

(Dated: August 1, 2018)

Neuronal systems have been modeled by complex networks in different description levels. Recently, it has been verified that networks can simultaneously exhibit one coherent and other incoherent domain, known as chimera states. In this work, we study the existence of chimera states in a network considering the connectivity matrix based on the cat cerebral cortex. The cerebral cortex of the cat can be separated in 65 cortical areas organised into the four cognitive regions: visual, auditory, somatosensory-motor and frontolimbic. We consider a network where the local dynamics is given by the Hindmarsh-Rose model. The Hindmarsh-Rose equations are a well known model of neuronal activity that has been considered to simulate membrane potential in neuron. Here, we analyse under which conditions chimera states are present, as well as the affects induced by intensity of coupling on them. We observe the existence of chimera states in that incoherent structure can be composed of desynchronised spikes or desynchronised bursts. Moreover, we find that chimera states with desynchronised bursts are more robust to neuronal noise than with desynchronised spikes.

PACS numbers: 05.45.Pq, 87.19.lj, 87.10.Hk

I. INTRODUCTION

The mammalian brain has neuronal mechanisms that give support to various anatomically and functionally distinct structures [1]. Mammals have the most complex brains of all vertebrates, which vary in size by a factor of 10^5 [2]. Such a brain is arranged according to not only interacting elements on different levels, but also of different interconnections and functions [3]. For instance, the cat has approximately 10^9 neurons in the brain and 10^{13} synapses [4, 5], while the human brain has approximately 10^{11} neurons and 10^{14} synapses [6].

One of the mammalian brain connectivity studies that has received considerable attention is the connectivity in the cat cerebral cortex [7, 8]. Scannell and Young [9] reported the connectional organisation of neuronal systems in the cat cerebral cortex. They arranged the cortex in four connectional groups of areas: visual, auditory, somatosensory-motor, and frontolimbic. Regarding this realistic neuronal network, it was studied the relationship between structural and functional connectivity at different levels of synchronisation [10]. Lameu et al. analysed bursting synchronisation [11] and suppression of phase synchronisation [12] in network based on cat's brain. They verified that the delayed feedback control can be an efficient method to have suppress synchronisation.

We focus on the existence of chimera states in a neuronal network model based on the cat cerebral cortex. Chimera states are spatiotemporal patterns in which coherent and incoherent domains mutually coexist [13, 14]. There are many studies about these patterns [15, 16].

Omel'chenko et al. observed chaotic motion of the chimera's position along arrays of nonlocally coupled phase oscillators, where the chimera states have no artificially imposed symmetry [17]. Chimera and phase-cluster states in populations of coupled chemical oscillators were studied by Tinsley et al. [18]. Considering coupled Belousov-Zhabotinsky oscillators, they verified that chimera lifetime grows approximately exponentially with system size. There are also experimental investigations about chimera states, e.g., in [19] demonstrated the existence of these patterns in an open chain of electronic circuits with neuron-like spiking dynamics. In addition, Martens et al. [20] showed the appearance of chimera states in experiments with mechanical oscillators coupled in a hierarchical network.

Coexistence of states was reported in several animals that exhibit conflict between sleep and wakefulness, where one cerebral hemisphere sleeps and the other stays in an awake condition [21]. Recently, Andrzejak et al. [22] demonstrated analogies between chimera state collapses and epileptic seizures. In neuronal systems, chimera states were found in a network of coupled Hodgkin-Huxley equations [23], and also in the C. Elegans brain network by coupling Hindmarsh-Rose equations [24, 25].

We build a neuronal network according to the matrix of corticocortical connections in the cat [8, 9]. In each cortical area we consider the neuron model proposed by Hindmarsh and Rose (HR) [26], and the axonal densities are considered as the connections between the areas. This neuronal network is able to reproduce EEG-like oscillations [27]. The HR neuron model can reproduce neuronal

activities such as regular or chaotic spikes, and regular or chaotic bursting [28]. Baptista et al. [29] analysed a HR neuronal network on the rate of information and synchronous behaviour. Hizanidis et al. [24] observed chimera states in nonlocally coupled HR neuron models, where each neuron is connected with its nearest neighbours on both sides. In this work, we consider unidirectional connections both inside each connectional group of area (intra) and between groups of areas (inter). Unidirectional connections can be related to chemical synapses [30]. As a result, we verify the existence of two kinds of chimera: spiking chimera (SC) with desynchronised spikes, and bursting chimera (BC) with desynchronised bursts. Moreover, we include a neuronal noise by adding a random term in the external current. This way, we demonstrate that BC is more robust to noise than SC.

Firstly, we introduce the neuronal network described by a coupled HR neuronal model. Then, we discuss our results about the existence of two kinds of chimera states and noise robustness. Finally, we draw our conclusions.

II. NEURONAL NETWORK

We consider a neuronal network composed for coupled HR according to the matrix that describes the corticocortical connectivity of the cat brain, obtained by Scannell et. al [8]. Fig. 1 shows the matrix of corticocortical connections in the cat brain with 1139 connections between 65 cortical areas which is organised into four cognitive regions: visual, auditory, somatosensory-motor and frontolimbic. In Ref. [8], the matrix was constructed by means of connections weighted 0, 1, 2, or 3, where 0 corresponds to absent of connections (white), 1 are sparse or weak (cyan), 2 are intermediate (orange), and connections weighted 3 are dense or strong (green).

The dynamic behaviour of the HR network is governed by the following equations

$$\begin{aligned} \dot{x}_j &= y_j - x_j^3 + bx_j^2 + I_j - z_j - \frac{\alpha}{n'} \sum_{k=1}^N G'_{j,k} \Theta(x_k) - \\ &\quad \frac{\beta}{n''} \sum_{k=1}^N G''_{j,k} \Theta(x_k), \\ \dot{y}_j &= 1 - 5x_j^2 - y_j, \\ \dot{z}_j &= \mu [s(x_j - x_{\text{rest}}) - z_j], \end{aligned} \quad (1)$$

where $\Theta(x_k) = (x_j - x_{\text{rev}})[1 + e^{-\lambda(x_k - \theta)}]^{-1}$, x_j is the membrane potential, y_j is related to the fast current (Na^+ or K^+), z_j is associated with the slow current (Ca^{2+}), b controls the spiking frequency, I_j corresponds to membrane input current ($1 \leq j \leq N$), x_{rev} is the reversal potential, λ and θ are sigmoidal function parameters, μ is responsible for the speed of variation of z , s governs adaptation, x_{rest} is the resting potential, α is the intra connection strength, $G'_{j,k}$ is the connection matrix of connections inside cortical areas (intra), β is the

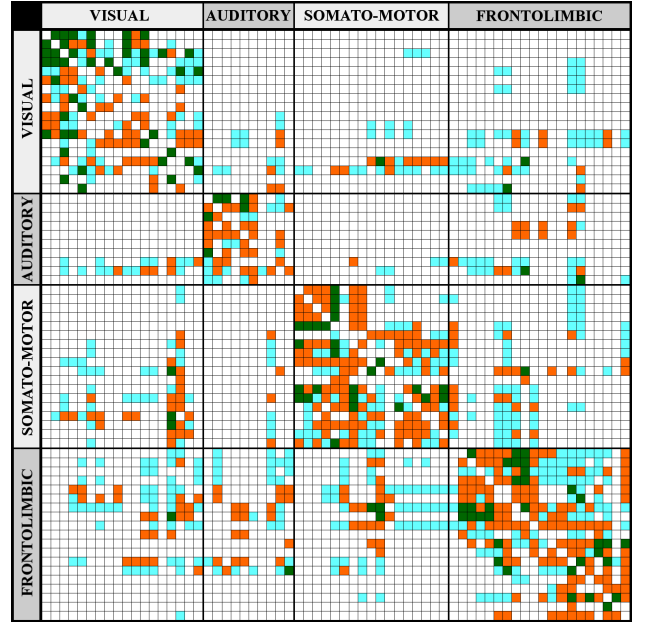


FIG. 1. (Colour online) Density of connections between cortical areas classified as absent of connection (white), sparse or weak (cyan), intermediate (orange), and dense or strong (green).

inter connection strength, and $G''_{j,k}$ is the connection matrix of connections between cortical areas (inter). We fix $b = 3.2$, $I_j = I_0 = 5.2$, $N = 65$ cortical areas, $x_{\text{rev}} = 2$, $\lambda = 10$, $\theta = -0.25$, $\mu = 0.01$, $s = 4.0$, and $x_{\text{rest}} = -1.6$ [25, 28]. The elements of the matrices $G'_{j,k}$ and $G''_{j,k}$ are 0 (absent of connection), 1/3 (weak), 2/3 (intermediate), or 1 (strong) according to the cat matrix (Fig. 1).

Fig. 2 shows space-time plots (left) and snapshot of the variable x (right). We use, in the snapshot, a colour for each cortical areas: visual in red, auditory in green, somatosensory-motor in blue, and frontolimbic in magenta. In Fig. 2a for $\alpha = 0.002$ and $\beta = 0.002$, the network has a desynchronous behaviour, namely it is not possible to observe a synchronised firing pattern. Consequently, the dynamics is spatially incoherent, as shown in Fig. 2b. For $\alpha = 0.3$ and $\beta = 0.1$, there is a clear synchronised firing pattern (Fig. 2c) and the network displays a spatially coherent dynamics (Fig. 2d).

III. CHIMERA STATES

One fact that has been verified is the coexistence of coherence and incoherence structures in networks [31]. This phenomenon in spatiotemporal dynamical systems is so-called chimera states [13]. Fig. 3 shows space-time plots (left) and snapshots (right) for different values of α and β in that it is possible to identify chimera states. In Figs. 3a and 3b for $\alpha = 0.7$ and $\beta = 0.12$, the somatosensory-motor area (blue) has a synchronous behaviour, namely it exhibits spatially coherent dynamics,

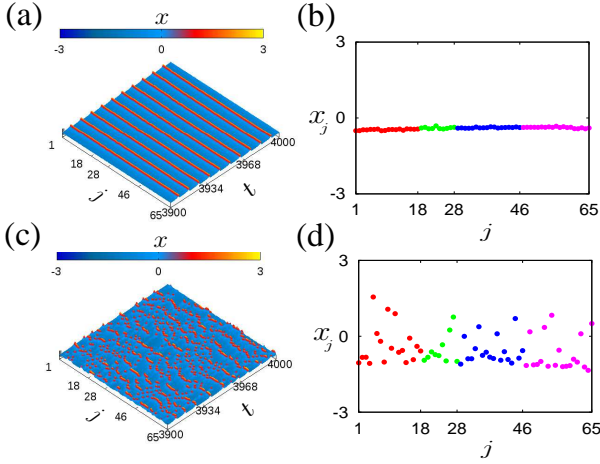


FIG. 2. (Colour online) Space-time plots (left) and snapshot of the variable x (right). (a) and (b) exhibit desynchronous behaviour for $\alpha = 0.002$ and $\beta = 0.002$. (c) and (d) show synchronous behaviour for $\alpha = 0.3$ and $\beta = 0.1$.

while the visual (red), the auditory (green) and frontolimbic (magenta) areas are spatially incoherent with bursting patterns. This chimera is SC because the incoherent intervals are characterized by desynchronised spikes. For $\alpha = 2.1$ and $\beta = 0.2$ (Figs. 3c and 3d), the auditory (green) and somatosensory-motor (blue) areas display synchronised patterns, whereas the other areas show incoherent structures. In this case, we verify BC, that is when desynchronised bursts are observed in the incoherent intervals.

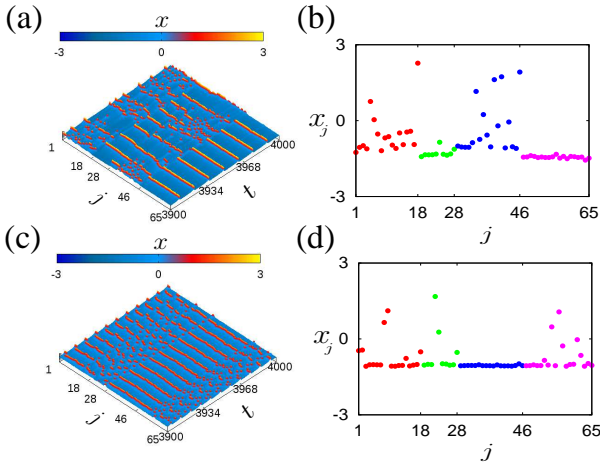


FIG. 3. (Colour online) Space-time plots (left) and snapshot of the variable x (right). (a) and (b) exhibit SC for $\alpha = 0.7$ and $\beta = 0.12$. (c) and (d) show BC for $\alpha = 2.1$ and $\beta = 0.2$.

As diagnostic tool we have used the metastability index and the chimera index [32]. To obtain these diagnostics, it is necessary to calculate Kuramoto's order parameter

[33], given by

$$\theta_m(t) = \left| \left\langle e^{i\phi_j(t)} \right\rangle_{j \in m} \right|, \quad (2)$$

where $m = 1$ (visual), 2 (auditory), 3 (somatosensory-motor), and 4 (frontolimbic), j is the neuron index, and ϕ_j is the neuronal phase defined as

$$\phi_j(t) = 2\pi k + 2\pi \frac{t - t_k}{t_{k+1} - t_k}, \quad (3)$$

t_k is the firing time of the j -th neuron. When $\theta_m(t) \approx 1$ the network displays a completely synchronous behaviour, however, when it is much less than 1 the phases are uncorrelated. Through θ_m , the chimera index and the metastability index are, respectively, given by [32]

$$\chi = \langle \sigma_{\text{chi}} \rangle_T, \quad (4)$$

and

$$\lambda = \langle \sigma_{\text{met}} \rangle_M, \quad (5)$$

where T is the time window for measurements and $M = 4$ (cortical areas),

$$\sigma_{\text{chi}}(t) = \frac{1}{M-1} \sum_{m \in M} [\theta_m(t) - \langle \theta(t) \rangle_M]^2, \quad (6)$$

and

$$\sigma_{\text{met}}(m) = \frac{1}{T-1} \sum_{t \leq T} [\theta_m(t) - \langle \theta_m \rangle_T]^2. \quad (7)$$

Figs. 4a and 4b show the parameter space $\beta \times \alpha$ for the chimera index and the metastability index, respectively. This way we can identify the regions where chimera states appear only by examining the difference between these two indexes. When the values of both χ and λ are low, the network is either synchronised or desynchronised [32]. The region A corresponds to low values of both χ and λ , and according to Figs. 2c and 2d we see that the neurons are synchronised. In addition, chimera states can be found when $\chi \gg \lambda$ [32]. As a result, the regions B and C correspond to chimera states (3), where χ is high and λ is low (Fig. 4). In addition, in the regions B and C we find SC and BC, respectively.

IV. NEURONAL NOISE

A relevant brain feature is noise, that can affect the transmission of signals and neuronal function [34]. There are many sources of noise in the brain, such as from genetic processes, thermal noise, ionic channel fluctuations, and synaptic events [35]. Serletis et al. [36] studied phase synchronisation of neuronal noise in mouse hippocampal. They reported from multi-spatial recordings that noise activity has a great influence on neurodynamic transitions in the healthy and epileptic brain.

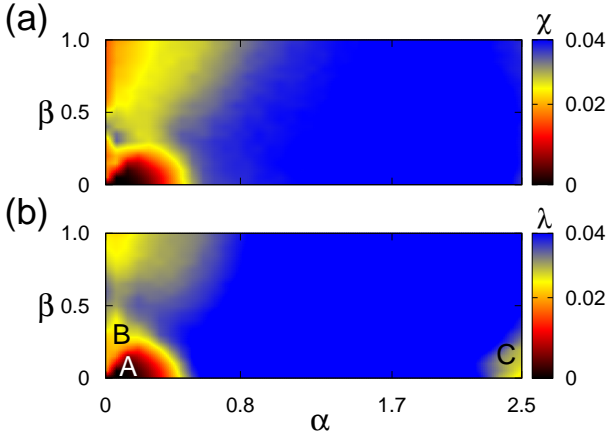


FIG. 4. (Colour online) Parameter spaces $\beta \times \alpha$ of the (a) chimera index χ and (b) the metastability index λ . Region A corresponds to low values of both χ and λ . Regions B and C denote $\chi \gg \lambda$ and there is the occurrence of chimera states.

We study the influence of neuronal noise on the chimera states in the cat brain. To do that, we consider an input current in Eq. 1 that is given by

$$I_j = I_0 + \delta \Psi_j, \quad (8)$$

where δ is the amplitude and Ψ_j is a normal distribution with mean 0 and variance 1 (Gaussian noise). For $\delta \geq 0$ the isolated neuron exhibits spiking pattern. There are many studies that consider neurons under the influence of Gaussian noise [37].

Fig. 5 shows the parameter spaces $\beta \times \alpha$ of the chimera index χ (left) and the metastability index λ (right) under an external current with noise (Eq. 8). For a small noise amplitude we do not observe significant alteration in the regions A (synchronous behaviour), B and C (chimera states), as shown in Figs. 5a and 5b for $\delta = 0.02$. However, when δ is increased it is possible to verify the destruction not only of synchronous behaviour, but also of chimera states. In Figs. 5c and 5d, where we consider $\delta = 0.1$, synchronisation and chimera states are completely suppressed.

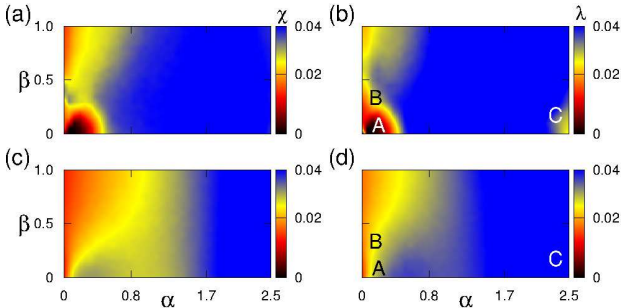


FIG. 5. (Colour online) Parameter spaces $\beta \times \alpha$ of the chimera index χ (left) and the metastability index λ (right) for different values of δ : (a) and (b) $\delta = 0.02$, and (c) and (d) $\delta = 0.1$.

We examine the robustness to noise of chimera states

with spiking and bursting structures. To do that, we vary the amplitude δ then we calculate χ and λ . The result in Fig. 6a corresponds to α and β into region B (Fig. 4), namely where the chimera has desynchronised spiking patterns. We see that for δ larger than about $\delta_1 = 0.03$, the χ -curve and the λ -curve have values that are approximately equal. Then, for $\delta \gtrsim \delta_1$ the noise suppresses the chimera states. The case when the chimera exhibits desynchronised bursting patterns (region C) is shown in Fig. 6b. As a result, there is an intersection point about $\delta_2 = 0.095$. Comparing the two points δ_1 and δ_2 , it is verified that $\delta_2 > \delta_1$. As a consequence, chimera states with desynchronised bursts are more robust to noise than with desynchronised spikes.

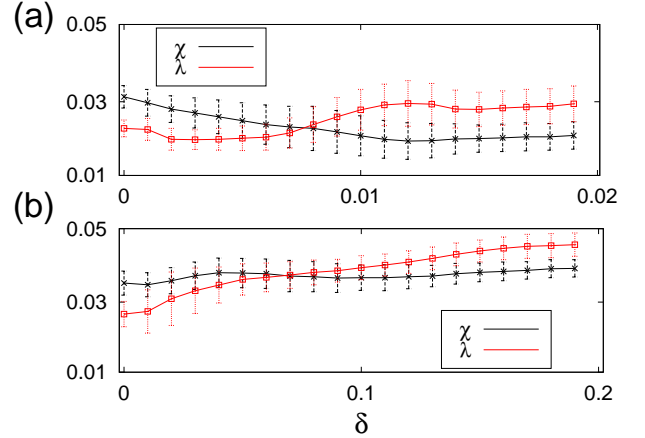


FIG. 6. (Colour online) χ (black line) and λ (red line) as a function of δ , where we consider (a) $\alpha = 0.7$ and $\beta = 0.1$ (desynchronised spikes), and (b) $\alpha = 2.1$ and $\beta = 0.2$ (desynchronised bursts). The bars correspond to the standard deviation calculated by means of 200 initial conditions.

V. CONCLUSIONS

We study a neuronal network composed by coupled HR model according to the connectivity matrix of the cat cerebral cortex. We consider unidirectional connections between neurons in the same area (intra) and between neurons in different areas (inter). This kind of connections can be associated with chemical synapses.

Varying the strength couplings, the network can exhibit synchronous and desynchronous behaviour. We also observe spatiotemporal patterns in that coherent and incoherent structures coexist, so-called chimera states. As diagnostic tool we use the chimera index and the metastability index to identify chimera states. As a result, we verify that the neuronal network model of the cat brain displays chimera states where the incoherent structures can be composed by desynchronised spikes or desynchronised bursts. SC occurs for small intra coupling strength, while BC appears for large intra coupling strength, and both for small inter coupling strength.

There are many sources of noise in the brain. With this in mind, we consider a noise in the external current to analyse effects on the chimera states. For small noise there is not significant changes in the parameter space ($\alpha \times \beta$) related to chimera, however, when the noise amplitude increases, chimera suppression is observed with the neuronal network exhibiting a desynchronous behaviour. In addition, we verify that BC is more robust to noise than SC.

ACKNOWLEDGMENTS

This study was possible by partial financial support from the following Brazilian government agencies: CNPq, CAPES, Fundação Araucária, and FAPESP (2015/07311-7 and 2011/19296-1), and IRTG 1740/TRP 2011/50151-0 funded by the DFG/FAPESP.

-
- [1] Barton R. A. and Harvey P. H., *Nature*, **405**, (2000) 1055.
 - [2] Willemet R., *Brain Sci.* **2**, 203 (2012).
 - [3] Zemanová L., Zhou C. and Kurths J., *Physica D*, **224** (2006) 202.
 - [4] Ananthanarayanan R., Esser S. K., Simon H. D., Modha, D. S., *IEEE - High Perform. Networking and Comp.*, **12** (2009) 1.
 - [5] Binzegger T., Douglas R. J., Martin K. A. C., *J. Neurosci.*, **29** (2004) 8441.
 - [6] Williams R. W., Herrup K., *Ann. Rev. Neurosci.*, **11** (1988) 423.
 - [7] Beul S. F., Grant S. and Hilgetag C. C., *Brain Struct. Funct.*, **220** (2015) 3167.
 - [8] Scannell J. W., Blakemore C. and Young M. P., *J. Neurosci.*, **15** (1995) 1463.
 - [9] Scannell J. W. and Young M. P., *Curr. Biol.*, **3** (1993) 191.
 - [10] Zhou C., Zemanová L., Zamora-López G., Hilgetag C. C. and Kurths J., *New J. Phys.*, **9** (2007) 178.
 - [11] Lameu E. L., Borges F. S., Borges R. R., Batista A. M., Baptista M. S. and Viana R. L., *Commun. Nonlinear Sci. Numer. Simul.*, **34** (2016) 45.
 - [12] Lameu E. L., Borges F. S., Borges R. R., Iarosz K. C., Caldas I. L., Batista A. M., Viana R. L. and Kurths J., *Chaos*, **26** (2016) 043107.
 - [13] Kuramoto Y. and Battogtokh D., *Nonl. Phen. Compl. Sys.*, **5** (2002) 380.
 - [14] Abrams D. M. and Strogatz S. H., *Phys. Rev. Lett.*, **93** (2004) 174102.
 - [15] Abrams D. M., Mirollo R., Strogatz S. H. and Wiley D. A., *Phys. Rev. Lett.*, **101** (2008) 084103.
 - [16] Ujjwal S. R., Punetha N. and Ramaswamy R., *Phys. Rev. E*, **93** (2016) 012207.
 - [17] Omel'chenko O. E., Wolfrum M. and Maistrenko Y. L., *Phys. Rev. E*, **81** (2010) 065201.
 - [18] Tinsley M. R., Nkomo S. and Showalter K., *Nature Phys.*, **8** (2012) 662.
 - [19] Gambuzza L. V., Buscarino A., Chessa S., Fortuna L., Meucci R. and Frasca M., *Phys. Rev. E*, **90** (2014) 032905.
 - [20] Martens E. A., Thutupalli S., Fourrière A. and Halatschek O., *PNAS*, **110** (2013) 10563.
 - [21] Rattenborg N. C., Amlaner C. J. and Lima S. L., *Neurosci. Biobehav. Rev.*, **24** (2000) 817.
 - [22] Andrzejak R. G., Rummel C., Mormann F. and Schindler K., *Sci. Rep.* **6** (2016) 23000.
 - [23] Sakaguchi H., *Phys. Rev. E*, **73** (2006) 031907.
 - [24] Hizanidis J., Kouvaris N. E. and Antonopoulos C. G., *Cibern. Phys.*, **4** (2015) 17.
 - [25] Hizanidis J., Kouvaris N. E., Zamora-López G., Dáz-Guilera A. and Antonopoulos C. G., *Sci. Rep.*, **6** (2016) 19845.
 - [26] Hindmarsh J. L. and Rose R. M., *Proc. Roy. Soc. B*, **221** (1984) 87.
 - [27] Schmidt G., Zamora-López G. and Kurths J., *Int. J. Bifurcat. Chaos*, **20** (2010) 859.
 - [28] Storace M., Linaro D. and Lange D., *Chaos*, **18** (2008) 033128.
 - [29] Baptista M. S., Moukan F. M. and Grebogi C., *Phys. Rev. E*, **82** (2010) 036203.
 - [30] Eccles J. C., *Ann. Rev. Neurosci.*, **5** (1982) 325.
 - [31] Santos M. S., Szezech Jr J. D., Batista A. M., Caldas I. L., Viana R. L. and Lopes S. R., *Phys. Lett. A*, **379** (2015) 2188.
 - [32] Shanahan M., *Chaos*, **20** (2010) 013108.
 - [33] Kuramoto Y., *Chemical Oscillations, Waves, and Turbulence*, (Springer Verlag, Berlin) 1984.
 - [34] Faisal A. A., Selen L. P. J. and Wolpert D. M., *Nature Rev.*, **9** (2008) 293.
 - [35] Destexhe A. and Rudolph-Lilith M., *Neuronal Noise*, (Springer Series in Computational Neuroscience, New York) 2012.
 - [36] Serletis D., Carlen P. L., Valiante T. A. and Bardakjian B. L., *Int. J. Neur. Syst.*, **23** (2013) 1250033.
 - [37] Lindner B., Longtin A. and Bulsara A., *Neural Comput.*, **15** (2003) 1761.